MOEM

Modern Electronic Materials 2024; 10(3): 145–152
DOI 10.3897/j.moem.10.3.131526

Research Article

Boron interaction with double-walled carbon nanotubes across temperature ranges

Utkir Uljayev[1,2], Shahnozakhon Muminova[1], Kamoliddin Mehmonov[1], Ishmumin Yadgarov[1], Abror Ulukmuradov[2]

1 Arifov Institute of Ion-Plasma and Laser Technologies, Academy of Sciences of Uzbekistan, 33 Durmon yuli Str., Tashkent 100125, Uzbekistan

2 Tashkent Institute of Textile and Light Industry, 5 Shakhdjakhon Str., Tashkent 100100, Uzbekistan

Corresponding author: Utkir Uljayev (utkir.uljaev@outlook.com)

Received 8 July 2024 ♦ **Accepted** 14 August 2024 ♦ **Published** 9 October 2024

Citation: Uljayev U, Muminova Sh, Mehmonov K, Yadgarov I, Ulukmuradov A (2024) Boron interaction with double-walled carbon nanotubes across temperature ranges. *Modern Electronic Materials* 10(3): 145–152. https://doi.org/10.3897/j.moem.10.3.131526

Abstract

Boron-adsorbing carbon nanotubes receive considerable attention in materials science due to their unique properties and potential applications. In particular, boron-adsorbing double-walled carbon nanotubes (DWNTs) exhibit a wide range of tunable electronic and optoelectronic properties. This study explores the influence of boron atoms on metallic (5,5@10,10) and semiconducting (8,0@17,0) DWNTs. We examine alterations in partial charge depending on the quantity of boron atoms adsorbed and affixed to the DWNT surface across temperatures from 300 K to 900 K. The results show that in both DWNTs, with the increase of energy corresponding to the temperature, the adsorption index of boron atoms (adsorbed to the first layer of DWNT) and the positive partial charge increase. Specifically, the maximum partial charge of DWNT(8,0)@(17,0) and DWNT(5,5)@(10,10) is 1.94*e* and 1.30*e* (at 300 K), 4.87*e* and 3.66*e* (at 600 K), 6.97*e* and 6.16*e* (at 900 K). Increasing boron concentration leads to heightened positive partial charge of DWNTs. This, in turn, affects the conductivity of the nanotube.

Keywords

double-walled carbon nanotube, boron adsorption, boron doping, reactive molecular dynamics

1. Introduction

Carbon nanotubes (CNTs), a class of carbon-based nanostructures, attract significant research attention, with literature on the subject expanding exponentially [1, 2]. These nanotubes, renowned for their distinctive properties, find extensive applications in microelectronics, energy storage, solar cells, sensors, cancer treatment, and drug delivery. They spark interest across multiple disciplines such as physics, chemistry, and materials science [3] their high mechanical strength, high specific surface area (SSA, demonstrating potential in electronic devices [4, 5], sensors [6] are safe, biocompatible, bioactive, and biodegradable materials, and have sparked a lot of attention due to their unique characteristics in a variety of applications, including medical and dye industries, paper manufacturing and water purification. CNTs also have a strong film-forming potential, permitting them to be widely employed in constructing sensors and biosensors. This review concentrates on the application of CNT-based nanocomposites in the production of electrochemical sensors and biosensors. It emphasizes the synthesis and optimization of CNT-based sensors for a range of applications and outlines the benefits of using CNTs for biomolecule immobilization. In addition, the use of molecularly imprinted polymer (MIP, material reinforce-

ment [7], adsorbents [8, 9] which is in high demand worldwide today, requires efficient hydrogen storage. Despite significant advances in hydrogen storage using carbon-based nanomaterials, including carbon nanotubes (CNTs, and various other domains [10]. Among them, double-walled carbon nanotubes (DWNTs) stand out due to their enhanced stability and mechanical properties [11, 12]. Comprising two coaxially aligned CNTs, DWNTs retain many of CNTs characteristics but possess greater physical robustness and electronic complexity [13]. Each DWNT consists of two concentric single-walled nanotubes (SWNTs) with a wall distance ranging from 0.33 to 0.42 nanometers [14]. The chiral indices of the inner and outer walls define DWNTs, with each wall being either a semiconductor (S) or a metal (M), resulting in four possible combinations (M@M, M@S, S@M, and S@S) [15]. Approximately 60% of all nanotube chiralities are semiconductors, while the remaining 40% are metals [15]. Various methods, including functionalization, offer means to tailor the properties of CNTs [16]. Functionalization, achieved through substitution reactions with similar heteroatoms or functional groups, alters CNTs solubility, chemical reactivity, and other physicochemical properties [17]. Notably, functionalization aids in the isolation of nanotube bundles. Consequently, studies have extensively explored DWNT interactions with atoms and molecules like boron (B) [18], nitrogen (N) [19], calcium (Ca) [20], palladium (Pd) [21], fluorine (F) [22], bromine [23], and platinum (Pt) [24]. In particular, D. Silambarasan et al. experimentally investigated hydrogen storage by functionalizing boron into single-walled carbon nanotubes [18]. Yann Tison et al. focused on the identification of nitrogen dopants in single-walled carbon nanotubes [19]. Silvia H. De Paoli Lacerda et al. studied how carbon nanotubes activate store-operated calcium entry in human blood platelets [20]. Huimin Wu et al. experimentally investigated the effects of fluorine-containing atoms and molecules on double-walled carbon nanotubes with various palladium [21]. L.G. Bulusheva and his colleagues have also contributed to this field [22]. In addition, L.G. Bulusheva and others examined the bromination of double-walled carbon nanotubes [23]. Dan Xia and others conducted experimental and modeling studies on extracting the inner wall from nested double-walled carbon nanotubes using platinum nanowires [24].

Despite considerable research, boron (B) and nitrogen (N) remain the preferred elements for substitution reactions [25, 26]. Boron serves as a *p*-type dopant and promotes nanotube growth while enhancing oxidation resistance [27]. The comparable atom sizes of boron and carbon facilitate their integration into the graphitic network. However, controlling the amount of boron (B) in the CNT structure remains a significant challenge. It has been reported that B promotes nanotube growth [28] and additionally that B increases the oxidation resistance [29]. Therefore, it appears that B possess complementary properties with regard to controlling nanotube morphology and properties. The similar atom sizes of boron and carbon facilitate their incorporation into the graphitic network. Although boron (B) atoms have been introduced into CNTs by various methods (e.g., CVD, ALD), controlling their amount in the structure is still one of the pressing problems [30, 31].

In this study, we investigated the changes in the charge distribution within the system as a result of adding boron atoms to Metal@Metal (M@M) and Semiconductor@Semiconductor (S@S) double-walled carbon nanotubes (DWNTs) at different temperatures and concentrations using molecular dynamics (MD) simulations.

2. Computational details

We investigate the process of boron (B) adsorption onto DWNTs through reactive MD simulations employing the LAMMPS package [32]. The ReaxFF potential describes interatomic interactions, accounting for bond breaking and formation [33]. Our model includes pristine Semiconductor@Semiconductor (S@S) (8,0)@(17,0) and Metal@Metal (M@M) (5,5)@(10,10) nanotubes, denoted as DWNT(8,0)@(17,0) and DWNT(5,5)@(10,10) in MD simulations (Fig. 1 (*a* and *b*)). Selected nanotubes' inner and outer diameters (0.682 and 1.364 nm for DWNT(8,0)@(17,0); 0.678 nm and 1.357 nm for DWNT(5,5)@(10,10)) fall within experimentally observed ranges (0.63–0.79 nm for inner; 1.3–1.6 nm for outer) [34, 35]. We apply periodic boundary conditions along the *z*-axis, allowing simulation of infinitely long DWNTs with lengths of 2.982 nm and 2.812 nm for DWNT(8,0)@(17,0) and DWNT(5,5)@(10,10) respectively.

Initially, we minimize the energy of all model systems using the conjugate gradient method. Subsequently, we equilibrate system temperature and pressure to desired values (300 K, 600 K, 900 K, and 0 Pa) in the NpT ensemble employing a Berendsen thermostat and barostat [36]. Our chosen heating rate (1 K/ps) aligns with previously reported values (0.1–10.0 K/ps) [37] ensuring insignificant deviations in thermodynamic equilibrium during temperature changes. For chemisorption of B atoms on DWNTs, we maintain system temperature at 300 K, 600 K, and 900 K for 100 ps using a Bussi thermostat [38].

In the simulations, the pressure of B atoms in the system is calculated as [39]

$$p = J\sqrt{\frac{2\pi MRT}{N_A}}, \tag{1}$$

where J is the impingement flux ($nm^{-2}\cdot ns^{-1}$); N_A is Avagadro's number, R is the universal gas constant; M is the molar mass of the B atom (kg/mol) and T is the temperature of the system (K). In this work, the impingement flux of the incident B atoms (i.e.,100 B) is 78.74 $nm^{-2}\cdot ns^{-1}$ (80.12 $nm^{-2}\cdot ns^{-1}$), and its corresponding pressure is ap-

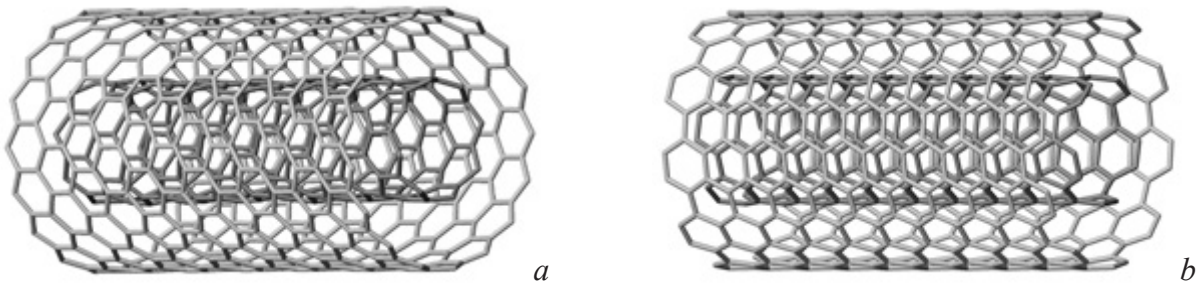

Figure 1. Side views of the DWNT(8,0)@(17,0) (*a*) and DWNT(5,5)@(10,10) (*b*) model system

proximately 1.94 MPa (1.97 MPa) for DWNT(5,5)@(10,10) (DWNT(8,0)@(17,0)). Simulations is conducted under NVT conditions, adding B atoms to the nanotube surface environment at 10 ps intervals, maintaining a minimum distance of 0.10 nm between each B atom and the model system.

We evaluate the adsorption coverage of B atoms remaining on pure DWNT surfaces under different temperatures (300 K, 600 K, 900 K) as:

$$\rho\% = N_B/N_C, \quad (2)$$

where, N_B is number of adsorbed boron (B) and N_C is number of carbon atoms.

In all cases MD time step is 0.1 fs. The simulations are conducted 5 times for each study case, and the results are obtained by averaging the corresponding physical quantities.

3. Results and discussion

When carbon nanotubes (CNTs) are grown with boron (B) at different temperatures, several factors come into play that can affect their structure, properties, and performance. From current literature, boron incorporation into carbon materials requires a high carbonization temperature of about 600–1100 °C [40–43]. The effect of boron on CNTs at low temperatures results in a high density of defects, leading to decreased electrical and thermal properties. Conversely, the addition of boron at high temperatures enhances thermal stability and improves electrical and mechanical properties [44]. Therefore, this study investigated the effect of boron on double-walled carbon nanotubes (DWNTs) at selected temperatures of 300 K, 600 K, and 900 K. The results indicate variations in the adsorption of B atoms on the surfaces of DWNT(8,0)@(17,0) and DWNT(5,5)@(10,10) at different temperatures (i.e., 300 K, 600 K, 900 K). At 300 K, 600 K, and 900 K, the maximum adsorption percentages (or adsorption coverage, ρ%) on DWNT(8,0)@(17,0) are 11.73%, 12.28%, and 14.14% respectively (Fig. 2*a*). The highest adsorption index is observed at 900 K, which is 1.17 and 1.15 times greater than at 300 K and 600 K. Similarly, for DWNT(5,5)@(10,10), the maximum ρ% values were 15.13%, 15.67%, and 15.84% at temperatures of 300 K, 600 K, and 900 K respectively (Fig. 2*b*). The largest adsorption index is at 900 K, which is 1.04 and 1.01 times greater than at 300 K and 600 K. It is evident that ρ% increases with temperature (from 0 eV to 10.0 eV).

The velocity (i.e., kinetic energy) of B atoms plays a significant role in their adsorption on DWNT(8,0)@(17,0) and DWNT(5,5)@(10,10) surfaces. Specifically, for DWNT(8,0)@(17,0) at 300 K, the adsorption

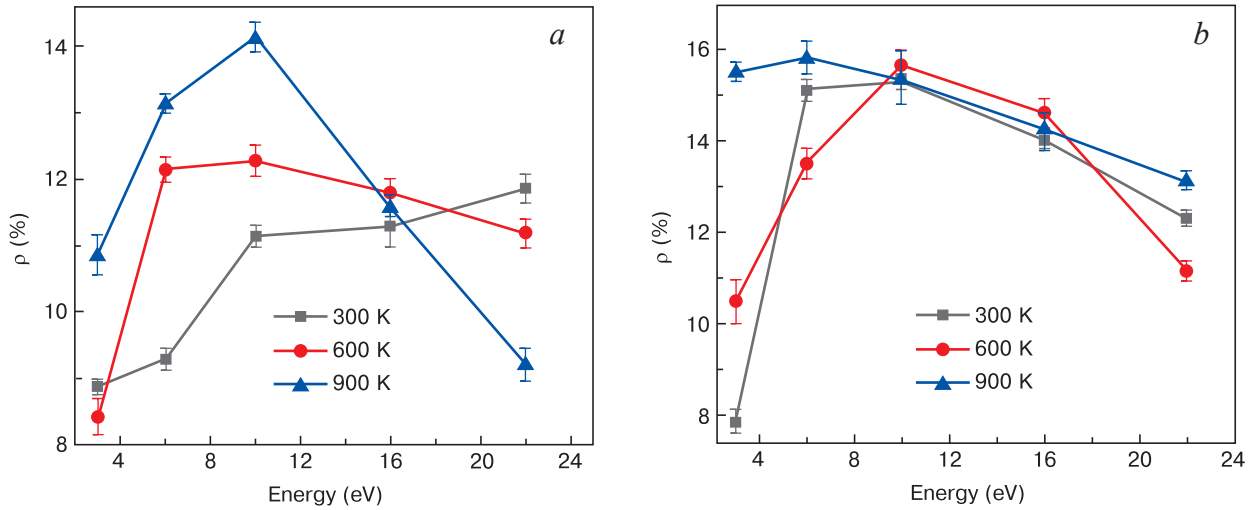

Figure 2. The relationship between the number of adsorbed boron (B) atoms and their kinetic energy is presented for DWNT(8,0)@(17,0) (*a*) and DWNT(5,5)@(10,10) (*b*) nanotubes

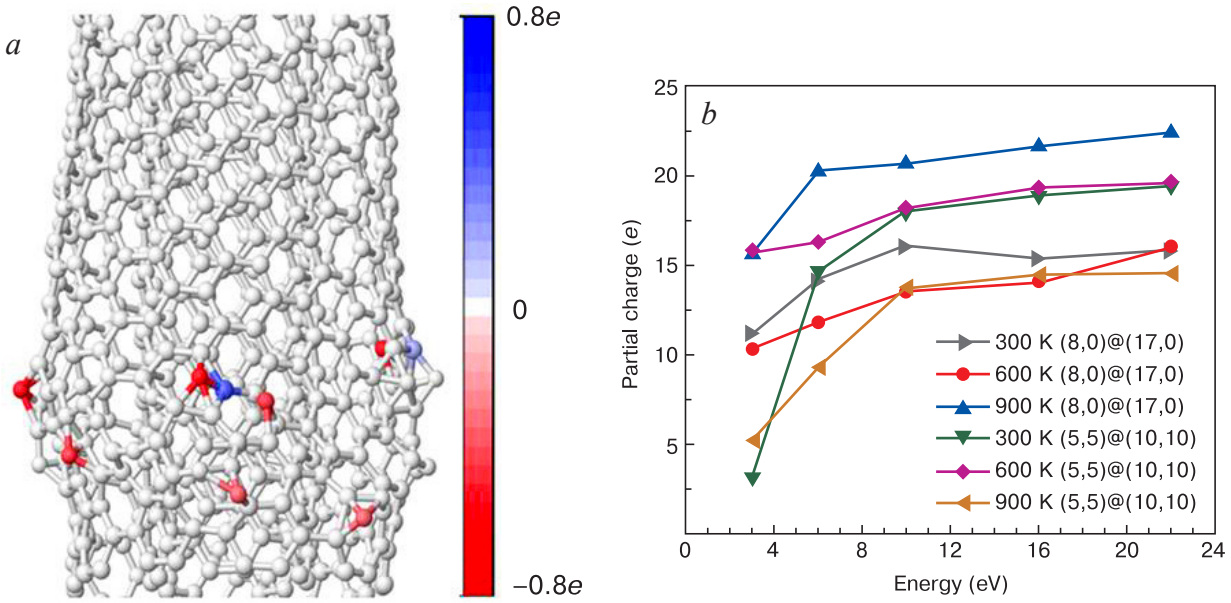

Figure 3. (*a*) Boron atoms chemisorbed onto DWNT(5,5)@(10,10) are introduced, and system atoms exhibit partial charges from –0.8*e* to +0.8*e*, which range from red to blue is depicted by the color spectrum, which shows the transition from electron-rich regions to electron-poor regions, respectively, (*b*) changes in partial charges on adsorbed B atoms as a result of deposition of boron atoms with different energies (different speeds) on double-walled carbon nanotubes at temperatures of 300 K, 600 K, 900 K

coverage increases as the velocity increases. However, at 600 K and 900 K, the adsorption rate steadily decreases (after 10 eV) after an initial increase (before 10 eV) (Fig. 2*a*, black line). Unlike DWNT(8,0)@(17,0) for DWNT(5,5)@(10,10) the same trend is observed at all temperatures. Initially, increases in B atom velocity (until ~8 eV) result in an increase in the adsorption level, but further increases in velocity (after ~8 eV) lead to a decrease in adsorption.

Various factors influence the chemisorption of B atoms on DWNTs, including the nanotube surface curvature and the arrangement of carbon rings [45, 46]. The adsorption index (adsorption coverage) varies with temperature, and depending on their position within the hexagonal cell of the CNT, B atoms may detach from the surface due to temperature effects [47, 48]. B atoms adsorbed on the surface of DWNTs are affected by the arrival of other B atoms on the surface. This can result in the formation of molecules through the Langmuir-Hinshelwood recombination mechanism, where two B atoms on the surface covalently bond to form a B molecule. Additionally, the presence of other B atoms on the surface can lead to molecular formation through mechanisms like Langmuir–Hinshelwood recombination or Eley–Rideal desorption. The temperature range (300–900 K) employed in this study alters the quantity of B atoms adsorbed on the surface [49, 50].

Atoms in the system are color-coded to represent positive charges in blue and negative charges in red, while uncharged atoms are depicted in white. The difference in electronegativity results in a variation in partial charges of carbon nanotube (CNT) and B atoms. Consequently, a relatively stronger interaction occurs between B atoms and DWNTs surfaces, leading to higher adsorption of B atoms. In this study, the charge distribution within the system changes according to the temperatures, corresponding to the adsorption coverage (ρ%) of B atoms with different energies adsorbed on the DWNT (first and second layers). Specifically, the sum of maximum partial charges of C atoms is approximately 1.61*e* (11.14%) and 1.81*e* (15.33%) for 300 K, 1.35*e* (12.28%) and 1.81*e* (15.67%) for 600 K, and 2.07*e* (14.14 %) and 0.93*e* (15.83%) for 900 K, respectively (Fig. 3*b*). This indicates that an increase in the concentration of B leads to an increase in positive partial charges of the DWNT. This validates the outcomes achieved in earlier investigations [30].

Boron atoms exhibit adsorption onto both the first and second layers of DWNTs depending on the insertion

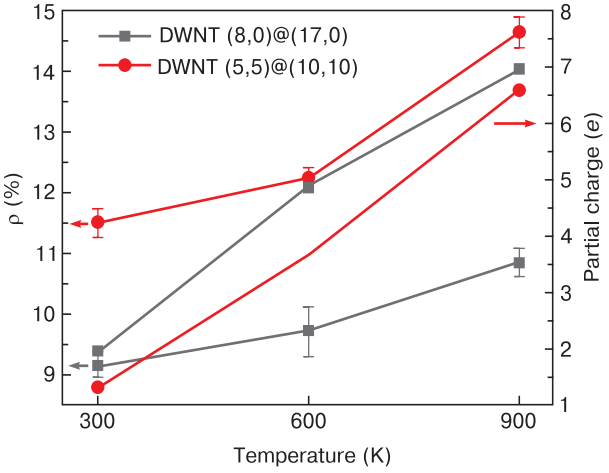

Figure 4. The maximal adsorption coverage as a function of temperature (left side), maximum partial charge for DWNT(8,0@17,0) and DWNT(5,5)@(10,10) (right side)

Table 1. Doping state of boron (B) atoms at different temperatures

Number B with doping	Partial charge (*e*)					
	DWNT (8,0)@(17,0)			DWNT (5,5)@(10,10)		
	300 K	600 K	900 K	300 K	600 K	900 K
1	1.02	1.73	1.88	0.07	0.40	2.16
3	1.18	3.47	2.91	0.14	1.45	3.29
7	2.16	4.88	3.26	1.09	2.70	3.40
10	2.43	4.93	3.72	2.09	3.63	3.55
15	4.19	5.42	4.01	3.32	3.99	4.02
20	6.48	5.81	4.46	4.64	4.70	4.07

energy level. As the insertion energy increases, a majority of the B atoms tend to adsorb onto the inner wall of the DWNTs. This process involves either replacing carbon atoms in the first layer (i.e., doping), pulling carbon atoms out of the system, or breaking the first layer and adsorbing onto the second layer [51, 52]. In our case, adsorbtion onto second wall of DWNT start at 6 eV energy of B atoms. Due to one of the primary objectives of our study is to assess changes in the electrical properties of the first layer of DWNTs without altering the properties of the second layer. Therefore, we conducted an analysis of the electrical properties (specifically, partial charge) associated with the adsorption of B atoms onto DWNTs at different temperatures, focusing on energy levels approximately within the range of 0–6 eV, which minimally impacts the second layer. Depending on the temperature applied to the system, B atoms adsorbed to the first layer at different energies are identified. Specifically, these maximal energies are 4 eV (9.14%), 4 eV (9.71%) and 3 eV (10.85%) for DWNT(8,0)@(17,0) and 4 eV (11.50%), 6 eV (13.16%) and 2 eV (14.66 %) for DWNT(5,5@10,10) at 300 K, 600 K and 900 K respectively (Fig. 4, left side). The partial charge corresponding to the maximum value of boron (B) atoms adsorbed to the first (upper) layer of nanotubes DWNTs is shown in Fig. 4 (right side). The maximum partial charge corresponding to this energy is 1.94*e* (4 eV), 4.87*e* (4 eV) and 6.97*e* (3 eV) for DWNT (8.0)@(17.0) and 1.30*e* (4 eV), 3.66*e* (6 eV) and 6.16*e* (2 eV) for DWNT(5,5)@(10,10).

Two DWNTs (i.e. 8,0@17,0 and 5,5@10,10) are doped with B atoms and subjected to different temperatures, then the changes in their partial charges (*e*) are compared (Table 1). The findings show that increasing the doping index of B atoms led to the corresponding result partial charge increase. This result is consistent with previous research findings [52]. B atoms are added (doped) to two DWNTs according to the maximum adsorption coverage (ρ%) and the partial charge (*e*) is compared. The partial charges of B atoms in DWNT(8,0@17,0) in the state of adsorption and doping (for temperatures of 300–900 K) are 1.94*e* (4 eV) and 5.97*e* for 300 K, 4.87*e* (4 eV) and 6.71*e* for 600 K, 6.97*e* (3 eV) and 12.51*e* for 900 K, while the partial charges for the DWNT(5,5)@(10,10) state are 1.30*e*, (4 eV) and 10.85*e* for 300 K, 3.66*e* (6 eV) and 11.08*e* for 600 K, 6.16*e* (2 eV) and 13.08*e* for 900 K, respectively. In this study, the average lengths of C–C and B–C bonds were found to be 0.143 and 0.152 nm, respectively, thus supporting the conclusion mentioned earlier [53, 54].

4. Conclusion

This molecular dynamics simulation effectively elucidated the adsorption mechanism of B on DWNT(8,0)@(17,0) and DWNT(5,5)@(10,10). The simulation revealed that the tendency (ρ%) of B adsorbed on DWNT(8,0)@(17,0) and DWNT(5,5)@(10,10) is affected by temperature factors. Specifically, the maximum ρ% of DWNT(8,0)@(17,0) at 300 K, 600 K, and 900 K are 12.03%, 12.28%, and 14.14%, respectively, while DWNT(5,5)@(10,10) – 15.13%, 15.67% and 15.84%. In addition to this, the charge distribution within the system varies with temperatures corresponding to the adsorption coverage (ρ%) of B atoms with different energies adsorbed on DWNT (first and second layers). In particular, the sum of the maximum partial charges of C atoms in DWNT(8,0)@(17,0) and DWNT(5,5)@(10,10) cases is about 1.61*e* (11.14%) for 300 K, respectively) and 1.81e (15.33%), 1.35*e* (12.28%) and 1.81*e* (15.67%) and 2.07*e* for 600 K, respectively. (14.14 %) and 0.93*e* (15.83 %) for 900 K, respectively. In conclusion, an increase in B concentration leads to an increase in the positive partial charges of DWNT. However, the overall effect is influenced by factors such as the type of nanotubes, the level and nature of doping, and temperature.

Acknowledgment

This research was carried out within the framework by the fundamental research program of the Academy Sciences of Uzbekistan. The simulations were performed using FISTUz cluster at the Institute of Ion-Plasma and Laser Technologies of the Academy of Sciences of Uzbekistan.

References

1. Iijima S. Carbon nanotubes: Past, present, and future. *Physica B Condensed Matter*. 2002; 323(1): 1–5. https://doi.org/10.1016/S0921-4526(02)00869-4
2. Rathinavel Sr., Priyadharshini K., Panda D. A review on carbon nanotube: An overview of synthesis, properties, functionalization, characterization, and the application. *Materials Science and Engineering B*. 2021; 268(3): 115095. https://doi.org/10.1016/j.mseb.2021.115095
3. Ali A., Rahimian Koloor S.S., Alshehri A.H., Arockiarajan A. Carbon nanotube characteristics and enhancement effects on the mechanical features of polymer-based materials and structures – A review. *Journal of Materials Research and Technology*. 2023; 24(5): 6495. https://doi.org/10.1016/j.jmrt.2023.04.072
4. Soto M., Boyer T.A., Biradar S., Ge L., Vajtai R., Elías-Zúñiga A., Ajayan P.M., Barrera E.V. Effect of interwall interaction on the electronic structure of double-walled carbon nanotubes. *Nanotechnology*. 2015; 26(16): 165201. https://doi.org/10.1088/0957-4484/26/16/165201
5. Peng L.-M., Zhang Z., Wang S. Carbon nanotube electronics: Recent advances. *Materials Today*. 2014; 17(9): 433. https://doi.org/10.1016/j.mattod.2014.07.008
6. Meskher H., Teqwa R., Thakur A.K., Ha S., Khelfaoui I., Sathyamurthy R., Sharshir S.W., Pandey A.K., Saidur R., Singh P., Jazi F.Sh., Lynch I. A review on CNTs-based electrochemical sensors and biosensors: Unique properties and potential applications. *Critical Reviews in Analitical Chemistry*. 2023; 54(7): 1–24. https://doi.org/10.1080/10408347.2023.2171277
7. Cui K., Chang J., Feo L., Chow C.L., Lau D. Developments and Applications of carbon nanotube reinforced cement-based composites as functional building materials. *Frontiers in Materials*. 2022; 9: 861646. https://doi.org/10.3389/fmats.2022.861646
8. Khalilov U., Uljayev U., Mehmonov K., Nematollahi P., Yusupov M., Neyts E. Can endohedral transition metals enhance hydrogen storage in carbon nanotubes? *International Journal of Hydrogen Energy*. 2024; 55: 604. https://doi.org/10.1016/j.ijhydene.2023.11.195
9. Sajid M., Asif M., Baig N., Kabeer M., Ihsanullah I., Mohammad A.W. Carbon nanotubes-based adsorbents: Properties, functionalization, interaction mechanisms, and applications in water purification. *Journal of Water Process Engineering*. 2022; 47(6348): 102815. https://doi.org/10.1016/j.jwpe.2022.102815
10. Kawasaki K., Harada I., Akaike K., Wei Q., Koshiba Y., Horike Sh., Ishida K. Complex chemistry of carbon nanotubes toward efficient and stable p-type doping. *Communications Materials*. 2024; 5: 21. https://doi.org/10.1038/s43246-024-00460-0
11. Ju S.-P., Lin J.-S., Chen H.-L., Hsieh J.-Y., Chen H.-T., Weng M.-H., Zhao J.-J., Liu L.-Z., Chen M.-C. A molecular dynamics study of the mechanical properties of a double-walled carbon nanocoil. *Computational Materials Science*. 2014; 82: 92. https://doi.org/10.1016/j.commatsci.2013.09.024
12. Zólyomi V., Koltai J., Rusznyák Á., Kürti J., Gali Á., Simon F., Kuzmany H., Szabados Á., Surján P.R. Intershell interaction in double walled carbon nanotubes: Charge transfer and orbital mixing. *Physical Review B. Condensed Matter*. 2008; 77(24): 245403. https://doi.org/10.1103/PhysRevB.77.245403
13. Green A., Hersam M. Properties and application of double-walled carbon nanotubes sorted by outer-wall electronic type. *ACS Nano*. 2011; 5: 1459–1467. https://doi.org/10.1021/nn103263b
14. Li Y., Wang K., Wei J., Gu Z., Wang Z., Luo J., Wu A. Tensile properties of long aligned double-walled carbon nanotube strands. *Carbon*. 2005; 43(1): 31–35. https://doi.org/10.1016/j.carbon.2004.08.017
15. Moore K.E., Tune D.D., Flavel B.S. Double-walled carbon nanotube processing. *Advanced Materials*. 2015; 27(20): 3105–3137. https://doi.org/10.1002/adma.201405686
16. Liu D., Shi L., Dai Q., Lin X., Mehmood R., Gu Z., Dai L. Functionalization of carbon nanotubes for multifunctional applications. *Trends in Chemistry*. 2024; 6(4): 186–210.
17. Adamska M., Narkiewicz U. Fluorination of carbon nanotubes − A review. *Journal of Fluorine Chemistry*. 2017; 200: 179–189. https://doi.org/10.1016/j.jfluchem.2017.06.018
18. Silambarasan D., Surya V.J., Vasu V., Iyakutti K. Experimental investigation of hydrogen storage in single walled carbon nanotubes functionalized with borane. *International Journal of Hydrogen Energy*. 2011; 36(5): 3574–3579. https://doi.org/10.1016/j.ijhydene.2010.12.028
19. Tison Y., Lin H., Lagoute J., Repain V., Chacon C., Girard Y., Rousset S., Henrard L., Zheng B., Susi T., Kauppinen E.I., Ducastelle F., Loiseau A. Identification of nitrogen dopants in single-walled carbon nanotubes by scanning tunneling microscopy. *ACS Nano*. 2013; 7(8): 7219. https://doi.org/10.1021/nn4026146
20. De Paoli Lacerda S.H., Semberova J., Holada K., Simakova O., Hudson S.D., Simak J. Carbon nanotubes activate store-operated calcium entry in human blood platelets. *ACS Nano*. 2011; 5(7): 5808–5813. https://doi.org/10.1021/nn2015369
21. Wu H., Wexler D., Liu H. Effects of different palladium content loading on the hydrogen storage capacity of double-walled carbon nanotubes. *International Journal of Hydrogen Energy*. 2012; 37(7): 5686–5690. https://doi.org/10.1016/j.ijhydene.2011.12.120
22. Bulusheva L.G., Fedoseeva Y.V., Flahaut E., Rio J., Ewels C.P., Koroteev V.O., Van Lier G., Vyalikh D.V., Okotrub A.V. Effect of the fluorination technique on the surface-fluorination patterning of double-walled carbon nanotubes. *Beilstein Journal of Nanotechnology*. 2017; 8(1): 1688–1698. https://doi.org/10.3762/bjnano.8.169
23. Bulusheva L.G., Okotrub A.V., Flahaut E., Asanov I.P., Gevko P.N., Koroteev V.O., Fedoseeva Yu.V., Yaya A., Ewels C.P. Bromination of double-walled carbon nanotubes. *Chemistry of Materials*. 2012; 24(14): 2708–2715. https://doi.org/10.1021/cm3006309
24. Xia D., Luo Y., Li Q., Xue Q., Zhang X., Liang C., Dong M. Extracting the inner wall from nested double-walled carbon nanotube by platinum nanowire: molecular dynamics simulations. *RSC Advances*. 2017; 7(63): 39480–39489. https://doi.org/10.1039/C7RA07066G
25. Uljaev U.B., Muminova S.A., Yadgarov I.D. Nitrogen adsorption on double-walled carbon nanotube at different temperatures: Mechanistic insights from molecular dynamics simulations. *East European Journal of Physics*. 2024; (1): 361–365.

26. Jana D., Sun C.-L., Chen L.-C., Chen K.-H. Effect of chemical doping of boron and nitrogen on the electronic, optical, and electrochemical properties of carbon nanotubes. *Progress in Materials Science.* 2013; 58(5): 565. https://doi.org/10.1016/j.pmatsci.2013.01.003
27. Li T.-J., Yeh M.-H., Chiang W.-H., Li Y.-Sh., Chen G.-L., Leu Y.-A., Tien T.-Ch., Lo Sh.-Ch., Lin L.-Y., Lin J.-J., Ho K.Ch. Boron-doped carbon nanotubes with uniform boron doping and tunable dopant functionalities as an efficient electrocatalyst for dopamine oxidation reaction. *Sensors and Actuators B Chemical*. 2017; 248: 288–297. https://doi.org/10.1016/j.snb.2017.03.118
28. Blase X., Charlier J.-C., De Vita A., Car R., Redlich Ph., Terrones M., Hsu W.K., Terrones H., Carroll D.L., Ajayan P.M. Boron-mediated growth of long helicity-selected carbon nanotubes. *Physical Review Letters*. 1999; 83(24): 5078. https://doi.org/10.1103/PhysRevLett.83.5078
29. Jones L.E., Thrower P.A. Influence of boron on carbon fiber microstructure. Physical properties, and oxidation behavior. *Carbon.* 1991; 29(2): 251–269. https://doi.org/10.1016/0008-6223(91)90076-u
30. Terrones M., Jorio A., Endo M., Rao A.M., Kim Y.A., Hayashi T., Terrones H., Charlier J.-C., Dresselhaus G., Dresselhaus M.S. New direction in nanotube science. *Materials Today*. 2004; 7(10): 16. https://doi.org/10.1016/S1369-7021(04)00628-5
31. Glerup M., Castignolles M., Holzinger M., Hug G., Loiseau A., Bernier P. Synthesis of highly nitrogen-doped multi-walled carbon nanotubes. *Chemical Communications.* 2003; 21(20): 2542–2543. https://doi.org/10.1039/b303793b
32. Thompson A.P., Aktulga H.M., Berger R., Bolintineanu D.S., Brown W.M., Crozier P.S., in't Veld P.J., Kohlmeyer A., Moore S.G., Nguyen T., Shan R., Stevens M.J., Tranchida J., Trott Ch., Plimpton S.J. LAMMPS – a flexible simulation tool for particle-based materials modeling at the atomic, meso, and continuum scales. *Computer Physics Communications*. 2022; 271(4): 108171. https://doi.org/10.1016/j.cpc.2021.108171
33. Mueller J.E., van Duin A.C.T., Goddard W.A.I. Development and validation of ReaxFF reactive force field for hydrocarbon chemistry catalyzed by nickel. *The Journal of Physical Chemistry C.* 2010; 114(11): 4939. https://doi.org/10.1021/jp9035056
34. Chen G., Bandow S., Margine E.R., Nisoli C., Kolmogorov A.N., Crespi V.H., Gupta R., Sumanasekera G.U., Iijima S., Eklund P.C. Chemically doped double-walled carbon nanotubes: Cylindrical molecular capacitors. *Physical Review Letters*. 2003; 90(25(Pt 1)): 257403. https://doi.org/10.1103/PhysRevLett.90.257403
35. Mehmonov K., Ergasheva A., Yusupov M., Khalilov U. The role of carbon monoxide in the catalytic synthesis of endohedral carbine. *Journal of Applied Physics*. 2023; 134(14): 144303. https://doi.org/10.1063/5.0160892
36. Berendsen H.J.C., Postma J.P.M, van Gunsteren W.F., DiNola A., Haak J.R. Molecular dynamics with coupling to an external bath. *The Journal of Chemical Physics.* 1984; 81: 3684. https://doi.org/10.1063/1.448118
37. Sun J., Liu P., Wang M., Liu J. Molecular dynamics simulations of melting iron nanoparticles with/without defects using a reaxff reactive force field. *Scientific Reports*. 2020; 10(1): 3408. https://doi.org/10.1038/s41598-020-60416-5
38. Bussi G., Donadio D., Parrinello M. Canonical sampling through velocity rescaling. *The Journal of Chemical Physics*. 2007; 126(1): 014101. https://doi.org/10.1063/1.2408420
39. Khalilov U., Bogaerts A., Neyts E.C. Microscopic mechanisms of vertical graphene and carbon nanotube cap nucleation from hydrocarbon growth precursors, *Nanoscale*. 2014; 6(15): 9206. https://doi.org/10.1039/c4nr00669k
40. Sharma A., Patwardhan A., Dasgupta K., Joshi J.B. Kinetic study of boron doped carbon nanotubes synthesized using chemical vapour deposition. *Chemical Engineering Science*. 2019; 207: 1341–1352. https://doi.org/10.1016/j.ces.2019.06.030
41. Keru G., Ndungu P.G., Nyamori V.O. Effect of boron concentration on physicochemical properties of boron-doped carbon nanotubes. *Materials Chemistry and Physics.* 2015; 153: 323–332. https://doi.org/10.1016/j.matchemphys.2015.01.020
42. Sawant S.V., Patwardhan A.W., Joshi J.B., Dasgupta K. Boron doped carbon nanotubes: synthesis, characterization and emerging applications – A review. *Chemical Engineering Journal*. 2022; 427(6348): 131616. https://doi.org/10.1016/j.cej.2021.131616
43. Monteiro F.H., Larrude D.G., Maia da Costa M.E.H., Terrazos L.A., Capaz R., Freire F. Production and characterization of boron-doped single wall carbon nanotubes. *The Journal of Physical Chemistry C.* 2012; 116(5): 3281–3285. https://doi.org/10.1021/jp209494z
44. Fakhrabadi M.M.S., Allahverdizadeh A., Norouzifard V., Dadashzadeh B. Effects of boron doping on mechanical properties and thermal conductivities of carbon nanotubes. *Solid State Communications*. 2012; 152(21): 1973–1979. https://doi.org/10.1016/j.ssc.2012.08.003
45. Ayala P., Grüneis Al., Gemming Th., Grimm D., Kramberger Ch., Rümmeli M.H., Freire F., Kuzmany H., Pfeiffer R., Barreiro A., Büchner B., Pichler Th. Tailoring *n*-doped single and double wall carbon nanotubes from a nondiluted carbon/nitrogen feedstock. *The Journal of Physical Chemistry.* 2007; 111(7): 2879. https://doi.org/10.1021/jp0658288
46. Su W., Li X., Li L., Yang D., Wang F., Wei X., Zhou W., Kataura H., Xie S., Liu H. Chirality-dependent electrical transport properties of carbon nanotubes obtained by experimental measurement. *Nature Communications.* 2023; 14(1): 1672. https://doi.org/10.1038/s41467-023-37443-7
47. Khalilov U., Bogaerts A., Xu B., Kato T., Kaneko T., Neyts E.C. How the alignment of adsorbed *ortho* H pairs determines the onset of selective carbon nanotube etching. *Nanoscale*. 2017; 9(4): 1653. https://doi.org/10.1039/C6NR08005G
48. Abdullah N.R., Rashid H.O., Kareem M.T., Tang C.-S., Manolescu A., Gudmundsson V. Effects of bonded and non-bonded B/N codoping of graphene on its stability, interaction energy, electronic structure, and power factor. *Physics Letters A*. 2020; 384(12): 126350. https://doi.org/10.1016/j.physleta.2020.126350
49. Sha X., Jackson B., Lemoine D. Quantum studies of Eley–Rideal reactions between H atoms on a graphite surface. *The Journal of Chemical Physics*. 2002; 116(16): 7158–7169. https://doi.org/10.1063/1.1463399
50. Zecho T., Güttler A., Sha X., Lemoine D., Jackson B., Küppers J. Abstraction of D chemisorbed on graphite (0001) with gaseous H atoms. *Chemical Physics Letters.* 2002; 366(1-2): 188–195. https://doi.org/10.1016/S0009-2614(02)01573-7

51. Muramatsu H., Kang C.-S., Fujisawa K., Kim J.H., Yang C.-M., Kim J.H., Hong S., Kim Y.A., Hayashi T. Outer tube-selectively boron-doped double-walled carbon nanotubes for thermoelectric applications. *ACS Applied Nano Materials*. 2020; 3(4): 3347. https://doi.org/10.1021/acsanm.0c00075

52. Pyawarai A.K. Simulating of boron atoms interacting with a (10,0) carbon nano tube: A DFT study. *International Journal of Physics*. 2020; 8(1): 29–34. https://doi.org/10.12691/ijp-8-1-5

53. Ni M.Y., Zeng Z., Ju X. First-principles study of metal atom adsorption on the boron-doped carbon nanotubes. *Microelectronics Journal.* 2009; 40(4): 863–866. https://doi.org/10.1016/j.mejo.2008.11.021

54. Boroznin S.V. Carbon nanostructures containing boron impurity atoms: Synthesis, physicochemical properties and potential applications. *Modern Electronic Materials*. 2022; 8(1): 23–42. https://doi.org/10.3897/j.moem.8.1.84317